Soft-to-hard mode transition in the dynamical dipole mode induced in dissipative heavy-ion collisions

M. Cabibbo

Laboratorio Nazionale del Sud and University of Catania, Via S. Sofia 62, I-95123 Catania, Italy

(Received 8 June 2006; revised manuscript received 26 October 2007; published 18 January 2008)

The collective dipole dynamics evolving in intermediate dinuclear systems with exotic shape and charge distributions formed in charge asymmetric fusion entrance channels are systematically studied by solving a microscopic transport Boltzmann-Nordheim-Vlasov (BNV) equation and analyzing the obtained dipole signal. The BNV analysis shows a typical transition in the dipole oscillation frequency related to a transition from soft-to-hard mode in the dynamical dipole mode. The relative pre-equilibrium γ-ray emission probability is also evaluated by using the classical bremsstrahlung approach. In particular, by using this approach an analytical formula that gives the time-dependent γ rate during the equilibration of the collective mode versus the statistical GDR is extrapolated. The results are in agreement with other models and the few existing experimental data.

DOI: 10.1103/PhysRevC.77.014608 PACS number(s): 24.30.Cz, 25.60.Pj, 25.70.Jj, 25.70.Lm

I. INTRODUCTION

The extra dipole radiation coming from fusion reactions with charge asymmetry in the entrance channel has been widely studied over the past several years both theoretically [1–4] and experimentally [5–7]. As it is well known, the dipole moment at the touching configuration point, which is a function of the differences in N/Z of the two colliding nuclei, generates a strong dipole amplitude responsible for the extra yield in the observed γ-ray spectra with respect to the statistical case.

The importance of the study of this pre-equilibrium dipole mode, the so-called dynamical dipole, is due to different reasons. (i) The extremely short mean lifetime ($\hbar/\Gamma_{\mathrm{GDR}} \cong$ 50 fm/c) of this collective mode makes it an ideal probe to study nuclear systems under extreme conditions. In particular, it permits the study of the structure of the intermediate system and the collisional and mean-field dynamics that characterize the compound nucleus formation time. (ii) The second reason is the possibility of obtaining independent information on the damping of the isovector collective mode in very excited nuclear systems and on the symmetry term of the nuclear force.

Recent theoretical models [2,3] show that the dependence of the extra dipole yield from the incident beam energy presents a typical "rise and fall" behavior, whose nature, related to the early stage dynamics of the reaction, was understood only from a qualitative point of view.

Therefore this physics requires a complete understanding of the early stage dynamics occurring in this kind of reactions. In particular a key question is the determination of the time corresponding to the start of the collective behavior [in the sense of the standard giant dipole resonance (GDR) mode].

To this end in the next section a fully microscopic analysis will be presented by solving the Boltzmann-Nordheim-Vlasov (BNV) equation for the system $^{16}\mathrm{O} + {}^{98}\mathrm{Mo}$ at two different energies. Then, by analyzing the obtained dipole signal the detailed features of the dipole dynamics, from the early stage up to the asymptotic behavior characterized by a full GDR collectivity, will be clarified.

Starting from this analysis, in Sec. III, we present a model that gives a quantitative prediction for the extra yield of GDR photons. By using this model, based on the classical bremsstrahlung approach, the above-mentioned "rise and fall" behavior for the extra yield versus the incident beam energy is nicely reproduced. Moreover, the obtained results are in perfect agreement with those obtained by Baran *et al*. [3]. Within this model we try to extend to the pre-equilibrium stage the standard statistical formula for the GDR γ ray emitted by an equilibrate nucleus. In particular we attempt to extract an analytical formula that gives the time-dependent pre-equilibrium γ rate not only during the compound nucleus stage (question partially solved by Chomaz *et al*. [1]) but also during the thermal pre-equilibrium stage of the precompound nucleus phase.

In this work we try to clarify each aspect of the dynamical dipole mode induced in the dissipative heavy-ion collisions. For this reason this work can be considered not only in agreement with but also complementary to that by Baran *et al*. [3].

II. BNV ANALYSIS

For a better understanding of the dynamics occurring in dissipative collisions initiated in charge asymmetric entrance channels, we performed a fully microscopic analysis for the system $^{16}\mathrm{O} + {}^{98}\mathrm{Mo}$ at $4A$ MeV and $8A$ MeV of incident beam energy. In both calculations the impact parameter b was put equal to zero. We stress that in this work all calculations are relative to central collisions ($b = 0$).

The calculations are obtained by solving the BNV transport equation with the help of the Twingo code [8]. This approach incorporates in a self-consistent way mean-field and two-body collisions dynamics [9,10]. We remind that quantum and thermal fluctuations are not explicitly included in our approach. Some fluctuations are due to the finite number of the test particles used in the simulations. To reduce these fluctuations the results presented here are obtained from an average over several events. For the mean field we have used

a Skyrme-like parametrization (see Refs. [8,11]), which well reproduces nuclear matter saturation properties.

At each time step we have extracted and analyzed from the BNV calculation the dipole moment in $\vec{r}$ space. The analyzed time range extends from the "strong absorption configuration"[1] to about 100 fm/c after the compound nucleus formation time ($t_{CN} \cong 120$ fm/c at $E_{inc} = 4A$ MeV, $t_{CN} \cong 80$ fm/c at $E_{inc} = 8A$ MeV [2]).

We observe that at the strong absorption configuration time ($t = 0$ in our time scale) a standard GDR distribution, in which protons and neutrons of the whole system are separated, cannot be present, but we have a molecular dipole distribution at this instant. It is then useful to decompose the total dipole $D_r^{tot}(t)$ as a sum of molecular dipole $D_r^{mol}(t)$ [12] and the correspondent residual dipole $D_r^{res}(t)$[2]

$$D_r^{tot}(t) = D_r^{mol}(t) + D_r^{res}(t). \tag{1}$$

We remember that we are dealing with the components along the beam axis of the considered dipole moments. Moreover, taking into account the above considerations and the meaning of strong absorption configuration we can write

$$D_r^{tot}(0) \cong D_r^{mol}(0). \tag{2}$$

The three dipole moments just defined are plotted in Fig.1. As we clearly see in both cases ($4A$ and $8A$ MeV beam energy) the first instants of the fusion path are dominated by the molecular dipole moment, which is characterized by a much lower frequency than the one of the residual dipole [$D_r^{res}(t)$]. Moreover, although the molecular dipole decreases, the residual one grows. The total dipole has the characteristic behavior just observed in other works [2].

We now try to visualize the amplitude of the two dipole components [$D_r^{mol}(t)$, $D_r^{res}(t)$] versus the time for a depeer understanding of their evolution. To this aim we operate some fits of the two dipoles extracted from the BNV calculations. We used the following functions:

$$D_r^{mol}(t) = A_0 \cos[t\omega(t) + \phi]e^{-\gamma t/2} \quad \text{at} \quad 4A \text{ MeV}$$
$$\omega(t) = \omega_1 + \omega_2(1 - e^{-\gamma_\omega t}) \tag{3}$$

$$D_r^{mol}(t) = A_0 \cos(\omega t + \phi)e^{-\gamma t/2} \quad \text{at} \quad 8A \text{ MeV} \tag{4}$$

for the molecular dipole, whereas we use

$$D_r^{res}(t) = A_0 \sin[t\omega(t)](e^{-\lambda_1 t} - e^{-\lambda_2 t})$$
$$\omega(t) = \omega_1 + \frac{\omega_2}{e^{\frac{t_0 - t}{d_0}} + 1}. \tag{5}$$

for the residual dipole at both beam energies.

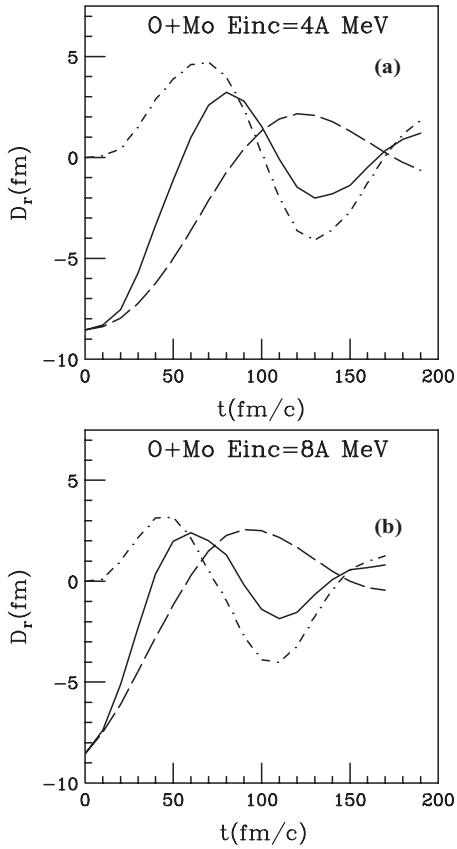

FIG. 1. BNV calculation of the three dipole moments discussed in the text for the system $^{16}O + ^{98}Mo$ at the two beam energies: total (full line), molecular (long-dashed line), and residual (dashed line).

The choice of function (4) for $D_r^{mol}(t)$ is quite natural if we observe Fig. 1(b). In this function the constant ϕ is introduced to take into account the initial dipole velocity. At $4A$ MeV it was necessary to introduce a time-dependent frequency[3] [$\omega = \omega(t)$ in Eq. (3)].

The residual dipole amplitude is modulated by the factor $(e^{-\lambda_1 t} - e^{-\lambda_2 t})$. We justify the introduction of this factor by analogy with the decay law. As it is well known in the decay phenomena this factor describes the evolution of the population of a daughter substance due to the decay of its parent. However, in our case, by analogy with the decay phenomena, we observe a trasformation of a molecular (mother) dipole $D_r^{mol}(t)$ into the residual (daughter) one $D_r^{res}(t)$.

The result of the fits are presented in Figs. 2(a) and 2(b). In these figures we have plotted the amplitude of the molecular dipole ($A_0^{mol}e^{-\gamma t/2}$) and of the residual one [$A_0^{res}(e^{-\lambda_1 t} - e^{-\lambda_2 t})$] at the two incident beam energies. From these plots we can confirm that the early stages ($t = 0 - \sim 60$ fm/c) are dominated by the molecular dipole that rapidly decreases and turns into a full GDR that we have called residual

[1] When the dinuclear system passes the strong absorption configuration the decision for fusion is taken. For light incident nuclei the strong absorption configuration is placed in the time scale just after the touching point configuration. In the following, i.e., in the calculation of the dipole amplitude at $t = 0$, we consider the two points as equivalent.

[2] The residual dipole is the sum of the dipole moments of the two reaction partners.

[3] We note that because we have only a very small variation of the frequency ω in $D_r^{mol}(t)$ [or in $D_r^{res}(t)$] the result of the fit is independent by the choice of the function $\omega = \omega(t)$, provided that we use a simple monotone function like $\omega = \omega(t)$ in Eq. (3) or Eq. (5).

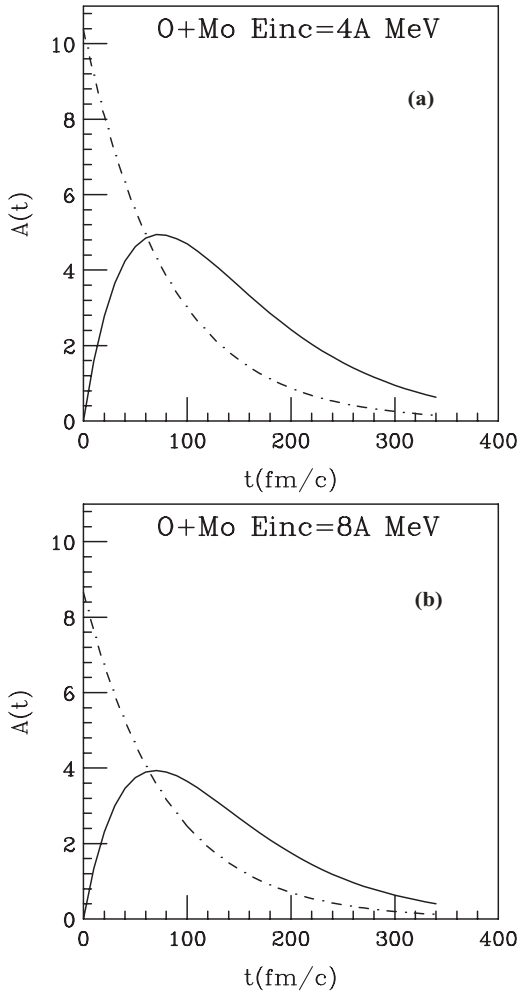

FIG. 2. Amplitude of the molecular dipole (dashed line) and of the residual one (full line) for the system $^{16}O + ^{98}Mo$ at the two beam energies (see text).

dipole. The point at which the two curves cross defines the start of the GDR behavior. This is about $t \cong 60$ fm/c in both cases.

From the results presented up to now (Figs. 1 and 2) we can extract some interesting information about the features of the dynamical dipole. In fact we conclude that the collective response effectively begins at $t = 0$ (strong absorption configuration), but the collective dynamics of the very early instants are very different from the standard GDR mode that in our description is represented by $D_r^{\rm res}(t)$. In the very early instants the collective dynamics is more similar to a soft-GDR where a fluid of ^{16}O oscillates against a fluid of ^{98}Mo. Moreover, the characteristic frequency is obviously less than the one related to the normal GDR mode [see Figs. 1(a) and 1(b)]. Because $D_r^{\rm res}(t)$ represents the proper GDR mode we can rewrite the total dipole as

$$D_r^{\rm tot}(t) = D_r^{\rm mol}(t) + D_r^{\rm GDR}(t). \tag{6}$$

In other words the collective dipolar evolution is a "mixing" of two modes: the molecular (soft mode) and the GDR (hard mode) one.

The given description can be regarded as a soft-to-hard mode transition in the dynamical dipole mode. In this scheme we can identify the time corresponding to the start of the GDR behavior as a transition time ($t_{\rm tr}$). Taking into account the values of the compound nucleus formation times at the two studied energies we can write

$$t_{\rm tr} \cong \frac{t_{\rm CN}}{2} \cong 60 \text{ fm}/c \quad \text{at} \quad 4A \text{ MeV} \tag{7}$$

$$t_{\rm tr} \cong \frac{3}{4} t_{\rm CN} \cong 60 \text{ fm}/c \quad \text{at} \quad 8A \text{ MeV}. \tag{8}$$

The existence of a transition from a soft mode to a hard one, which are characterized by different values of the frequency, suggests that the frequency of the total dipole $D_r^{\rm tot}(t)$ should show a strong variation, changing from the lower value of the molecular configuration to the higher value characterizing the GDR standard mode. To extrapolate the trend of the frequency $\omega(t)$ of the total dipole, we have fitted this dipole by using:

$$D_r^{\rm tot}(t) = A_0 \cos[t\omega(t)]e^{-\gamma t/2}, \tag{9}$$

where we have parameterized the function $\omega(t)$ with the following different functions:

$$\begin{aligned} \omega_a(t) &= \omega_1 + \omega_2(1 - e^{-\gamma_\omega t}) \\ \omega_b(t) &= Sa^{b^t} \\ \omega_c(t) &= \omega_1 + \frac{\omega_2}{e^{\frac{t_0 - t}{d_0}} + 1}. \end{aligned} \tag{10}$$

We observe that the behavior of the function $\omega_b(t)$ is similar to a Fermi function $\omega_c(t)$. In particular S represents the asymptotic value of the frequency ($S = \omega_\infty$), whereas the product $S \times a$ represents its initial value [$Sa = \omega_b(0)$].

We obtained good fits with all three functions. But the best fits were obtained with the function $\omega_b(t)$. The results of these fits are:

$$A_0 = -8.967 \quad \gamma = 0.02292 \quad S = 0.04844$$
$$a = 0.07794 \quad b = 0.9722$$

at $4A$ MeV, whereas we have, respectively,

$$A_0 = -8.539 \quad \gamma = 0.03292 \quad S = 0.05745$$
$$a = 0.3066 \quad b = 0.9697$$

at $8A$ MeV of incident beam energy.

In Figs. 3(a) and 3(b) the extracted frequency $\omega(t)$ of the total dipole is plotted. The results are relative to the fits obtained with the function $\omega_a(t)$[Fig. 3(a)] and with the function $\omega_b(t)$ [Fig. 3(b)].

As it was supposed, the frequency rapidly grows from a value of about 1–2.5 MeV up to the asymptotic value (10–11 MeV) characterizing the full GDR behavior. We can identify the lower value [$\omega(0) \cong$ 1–2.5 MeV] with the frequency of the molecular dipole. We observe that at $4A$ MeV of incident energy a net transition in frequency is evident [see dashed line in Fig. 3(b)]. In this case the relation (7) ($t_{\rm tr} \cong t_{\rm CN}/2$) is verified if we identify this time with the point where the frequency is halfway between the initial and the asymptotic value. We stress that the best fits are those presented in Fig. 3(b); so we can assume that the function $\omega_b(t)$ describes the behavior of the frequency.

In the next section we try to extract from the results presented in Fig. 3 an "effective frequency transition time"

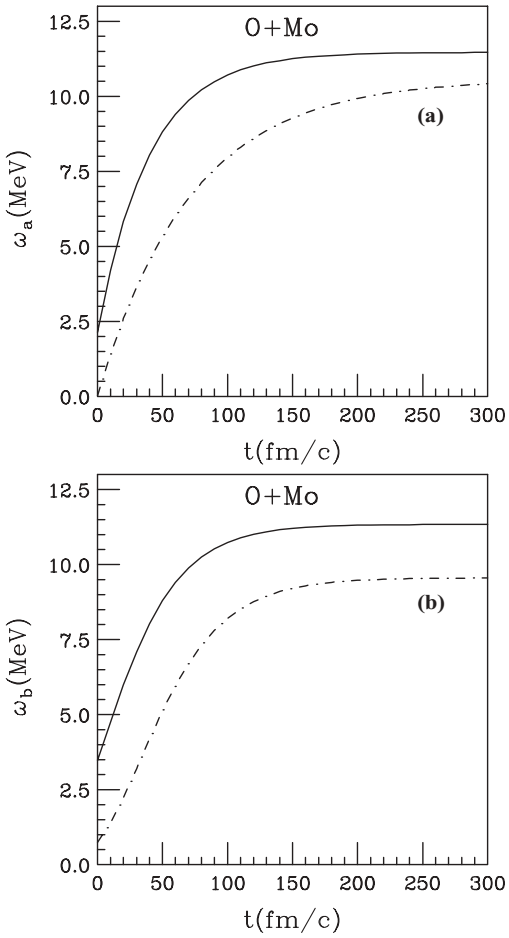

FIG. 3. Frequency of the total dipole as a function of the time by using ω_a and ω_b (see text) for the system $^{16}O + ^{98}Mo$ at $E_{inc} = 4A$ MeV (dashed line) and $E_{inc} = 8A$ MeV (full line).

that will be the starting point of a model for a quantitative prediction of the γ-ray extra yield.

III. PRE-EQUILIBRIUM γ-RAY EMISSION PROBABILITY

In this section we try to perform a model for a quantitative estimation of the pre-equilibrium γ-ray extra yield and its evolution with the incident beam energy.

We start adopting a sharp cut-off approximation for the total dipole frequency behavior. In particular we will write

$$\omega(t) = \begin{cases} 0 & \text{for} \quad t < \tilde{t}_{tr}, \\ \omega_\infty & \text{for} \quad t \geqslant \tilde{t}_{tr}, \end{cases} \tag{11}$$

where ω_∞ is the asymptotic value of the frequency. Moreover, the time $\tilde{t}_{tr}$ is an effective frequency transition time that we will try to extrapolate from the plots of Fig. 3. Such sharp cut-off approximation is justified within the classical electrodynamics. In fact the very low frequency characterizing the molecular phase ensures the negligibility of γ emission during this phase.

The time $\tilde{t}_{tr}$ can be derived by using a different method depending on the function $\omega(t)[\omega_a(t)$ or $\omega_b(t)]$ plotted in Fig. 3. In the case of the function $\omega_b(t) = Sa^{b^t}$ this instant can be identified with the point where the frequency is halfway between the initial and the asymptotic value. In the case of the function $\omega_a(t)$ we choose the time $\tilde{t}_{tr}$ so that the jump between the initial and the asymptotic frequency is reduced to $1/e$ of its initial value [which is $\Delta\omega(0) = \omega_2$].

We find that at $4A$ MeV the two methods just described, depending on the two cases [$\omega_a(t)$ or $\omega_b(t)$], give with good approximation the same value for the time $\tilde{t}_{tr}$, that is

$$\tilde{t}_{tr} \cong 60 \text{ fm}/c \quad E_{inc} = 4A \text{ MeV}. \tag{12}$$

Also at $E_{inc} = 8A$ MeV the two method are fully consistent. We find in this case

$$\tilde{t}_{tr} \cong 40 \text{ fm}/c \quad E_{inc} = 8A \text{ MeV}. \tag{13}$$

Remembering the compound nucleus formation time at the two incident beam energies, we can summarize the two results (12) and (13) in the single expression

$$\tilde{t}_{tr} \cong \frac{t_{CN}}{2}. \tag{14}$$

In other words, in the analyzed energy range, the effective frequency transition time corresponds approximatively to half the compound nucleus formation time. Moreover, we observe from Fig. 1 that the effective frequency transition time of Eq. (14) approximatively coincides with the first zero of the total dipole $D_r^{tot}(t)$ in both cases of Fig. 1.

It should not come as a surprise that $\tilde{t}_{tr}$ coincides with t_{tr} only at the incident energy $4A$ MeV. In fact there is no reason that the two times t_{tr} and $\tilde{t}_{tr}$ are exactly coincident, especially at $8A$ MeV, when the transition becomes less abrupt [see full line in Fig. 3(b)]. In this case $\tilde{t}_{tr}$ is only an "effective" transition time in the context of our calculation. For these reasons we base our model on the simple relation (14) that we assume valid also at higher energies.

To evaluate the pre-equilibrium γ-ray emission probability we start from the bremsstrahulung formula [3,13] ($E_\gamma = \hbar\omega$)

$$\frac{dP}{dE_\gamma} = \frac{2e^2}{3\pi\hbar c^3 E_\gamma}\left(\frac{NZ}{A}\right)^2 |\ddot{x}(\omega)|^2, \tag{15}$$

which gives the total emission probability. In this classical approach $\ddot{x}(\omega)$ is the Fourier trasform of the acceleration $\ddot{x}(t)$ associated with the distance between the center of mass of protons (Z) and neutrons (N) of the whole system [$x(t) = R_z(t) - R_n(t)$]

$$\ddot{x}(\omega) = \int_0^\infty \ddot{x}(t) e^{i\omega t} dt. \tag{16}$$

If we assume, coherently with the cut-off approximation [Eqs. (11) and (14)] for the frequency, a full GDR behavior for $t \geqslant t_{CN}/2$, we can identify in the range of time $(t_{CN}/2, \infty)$ the distance function $x(t)$ as a solution of the following Langevin-type of equation

$$\ddot{x}(t) + \gamma\dot{x}(t) + \omega_0^2 x(t) = \frac{F_r(t)}{M_{coll}}; \quad t \geqslant t_{CN}/2, \tag{17}$$

where $M_{coll} = \frac{NZ}{A}m$ is the reduced mass of the neutron-proton relative motion, γ is the dissipation constant related to the width ($\gamma = \Gamma^\downarrow/\hbar$), and $\omega_0 \equiv \omega_\infty$ is the asymptotic proper frequency. Finally $F_r(t)$ is a fictitious random force that

simulates the interaction of our GDR oscillator with the CN heat bath.

Actually in the interval $t_{CN}/2 \leqslant t < t_{CN}$ the thermal equilibrium is not yet reached, so during this interval the features of the random force $F_r(t)$ are in general different from those relative to the equilibrium case. But, as discussed later, we can assume the interval $t_{CN}/2 \leqslant t < t_{CN}$, from a thermal point of view, as a quasiequilibrium phase. Consequently, during this phase the features of the random force $F_r(t)$ can be assumed to be very close to those of the equilibrium case. Thus during the considered range $(t_{CN}/2 \leqslant t < \infty)$ we can refer with a good approximation to the CN heat bath to determine $F_r(t)$.

The possibility to assume a quasiequilibrium situation during the pre-CN phase $(t_{CN}/2 \leqslant t < t_{CN})$ can be evidenced by solving a very simple Boltzmann kinetic equation $\partial g(\vec{p})/\partial t = I[g]$ for the impulse microscopic distribution function $g(\vec{p})$. In fact with a simple linearization of the collision integral $I[g]$ we find that the distribution function $g(\vec{p})$ goes to equilibrium following the exponential factor $(1 - e^{-t/t_{CN}})$. This typical behavior confirms the validity of the above approximations.

Assuming small values for the spreading width $(\gamma \to 0)$ we can write the solution of Eq. (17) as

$$x(t) \cong x_1(t) + x_r(t); \quad t \geqslant t_{CN}/2, \tag{18}$$

where

$$x_1(t) = x_{tp} \sin(\omega_0 t - \omega_0 t_{CN}/2 + \psi) e^{-\gamma t/2}. \tag{19}$$

The first term $x_1(t)$ of Eq. (18) is the solution of the associated homogeneous equation. The second term $x_r(t)$ is the stationary solution of Eq. (17). In the first term the factor x_{tp} is the amplitude of the function $x_1(t)$ at the touching point.

The phase ψ [Eq. (19)] has been introduced to reproduce the boundary condition at $t = t_{CN}/2$. We remember that Eqs. (18) and (19) describe the motion for $t \geqslant t_{CN}/2$. By using this solution we suppose a full stability at the transition time $(t_{CN}/2)$. In other words we assume for the random-type solution $x_r(t)$ a stationary behavior for $t \geqslant t_{CN}/2$. In effect, because the random force $F_r(t)$ starts to act just at $t = t_{CN}/2$, the function $x_r(t)$ will take some time before reaching stability. Postponing the analysis of this delay effect we shall assume, for the moment, the ideal conditions just outlined to simplify the mathematical description.

Finally, taking into account the cut-off approximation in Eq. (11), we shall assume as the basic solution of our model the following distance function

$$x(t) = \begin{cases} x_1(t) + x_r(t) & \text{for} \quad t \geqslant t_{CN}/2, \\ 0 & \text{for} \quad t < t_{CN}/2. \end{cases} \tag{20}$$

The Fourier trasform of the acceleration [Eq. (16)] will then be written as

$$\ddot{x}(\omega) = \int_{t_{CN}/2}^{\infty} [\ddot{x}_1(t) + \ddot{x}_r(t)] e^{i\omega t} dt. \tag{21}$$

By suitably regulating procedure one can show that

$$\langle |\ddot{x}(\omega)|^2 \rangle = |\ddot{x}_1(\omega)|^2 + \lim_{T_0 \to \infty} \omega^4 T_0 |\alpha(\omega)|^2 \left(F_r^2\right)_\omega, \tag{22}$$

where the average $\langle \cdot \rangle$ refers to the statistical ensemble. Moreveor $\alpha(\omega) = 1/M_{coll}(\omega_0^2 - \omega^2 - i\gamma\omega)$ and $(F_r^2)_\omega$ is the spectral density of the mean-square fluctuations of the random force (see also Ref. [3]). Taking into account the above considerations on the possibility to assume a quasiequilibrium behavior during the interval $(t_{CN}/2, t_{CN})$, we can apply the fluctuation-dissipation theorem [14]. So we have $(E_\gamma = \hbar\omega)$

$$\begin{aligned} \left(F_r^2\right)_\omega &= M_{coll}\, \omega \Gamma^{\downarrow} \coth\left(\frac{\hbar\omega}{2T}\right) \\ &\cong M_{coll}\, \omega \Gamma^{\downarrow} (2e^{-E_\gamma/T}), \end{aligned} \tag{23}$$

where the approximation (second equation) was obtained excluding the zero-point motion and expanding the hyperbolic function for $\hbar\omega > T$.

By inserting Eq. (22) into Eq. (15) we obtain the total γ-ray emission probability, which will consist of two terms

$$\frac{dP}{dE_\gamma} = \frac{dP^{(1)}}{dE_\gamma} + \frac{dP^{(r)}}{dE_\gamma}, \tag{24}$$

The first term is the extra dipole contribution. It is the "direct" dipole contribution due to the presence of a charge asymmetry in the entrance channel. The top index (1) indicates that the total probability $dP^{(1)}/dE_\gamma$ is evaluated by introducing the first term of Eq. (22) into Eq. (15). We will evaluate this term later. The second term $[dP^{(r)}/dE_\gamma]$ is the background thermal contribution. By introducing the second term of Eq. (22) into Eq. (15) and by using Eq. (23) we evaluate $dP^{(r)}/dE_\gamma$ as

$$\begin{aligned} \frac{dP^{(r)}}{dE_\gamma} &= \lim_{T_0 \to \infty} T_0 \frac{dR^{(r)}}{dE_\gamma} \\ &\cong \lim_{T_0 \to \infty} T_0 \frac{1}{\hbar} \frac{E_\gamma^2}{(\pi\hbar c)^2} \frac{\sigma_{abs}}{3} e^{-E_\gamma/T}, \end{aligned} \tag{25}$$

where, by using the fluctuation-dissipation theorem [Eq. (23)], we have evidenced the background thermal rate $dR^{(r)}/dE_\gamma$.

As we can see this contribution coincides with the standard statistical formula for the GDR γ ray emitted by an equilibrate nucleus. We stress that this coincidence in the interval $(t_{CN}/2, t_{CN})$ is not casual but, as discussed before, is related to the possibility of assuming in this interval the features of the random force $F_r(t)$ close to the equilibrium case and consequently to the possibility of using the fluctuation-dissipation theorem [Eq. (23)]. By using this theorem we assume, as a first approximation, that these features coincide with the CN ones and are independent of the time. In particular the temperature T that appears in Eq. (25) represents the CN temperature.

Let us now evaluate the first term of Eq. (24). To this end we start to calculate $\ddot{x}_1(\omega) = \int_{t_{CN}/2}^{\infty} \ddot{x}_1(t) e^{i\omega t} dt$. For this calculation we use Eqs. (20) and (19) for $x_1(t)$. In Eq. (19) we can set to zero the phase ψ. In fact, as observed above in Figs. (1), at both incident energies the instant $t = t_{CN}/2$ coincides with good approximation with the first zero of the total dipole $D_r^{tot}(t)$ [and then $x_1(t)$]. With this condition we have $x_1(t_{CN}/2) = 0$. Then, because we have assumed above in Eq. (20) $x_1(t) = 0$ for $t < t_{CN}/2$, we have, after a double integration by parts:

$$\ddot{x}_1(\omega) = -\dot{x}_1(t_{CN}/2) e^{i\omega t_{CN}/2} - \omega^2 x_1(\omega), \tag{26}$$

where $x_1(\omega) = \int_{t_{CN}/2}^{\infty} x_1(t) e^{i\omega t} dt$. At this point, taking into account that:

(i) in the region of the resonance [which is described by the second term of Eq. (26)] the first term of the Eq. (26) is negligible with respect the second one and
(ii) from the demonstration of Eq. (26) it follows that the first term of this equation is related to the discontinuity in $\dot{x}_1(t)$ at $t = t_{CN}/2$

and taking also into account that in reality no discontinuity is present in $\dot{x}_1(t)$, it is reasonable to cut the first term in Eq. (26). Finally we have

$$\ddot{x}_1(\omega) = -\omega^2 x_1(\omega). \tag{27}$$

We stress that this procedure is not an approximate evaluation of $\ddot{x}_1(\omega)$ [Eq. (26) is in fact an exact result] but rather a simplification in the calculation of the integral that allows us to free $\ddot{x}_1(\omega)$ from those nonrealistic contributions originating from the sharp cut-off approximation assumed before.

Finally, the first term of Eq. (24) can be obtained by introducing $|x_1(\omega)|^2$ (multiplied for ω^4) into Eq. (15). We have

$$\frac{dP^{(1)}}{dE_\gamma} = x_0^2 \frac{e^2}{6\pi(\hbar c)^3}\left(\frac{NZ}{A}\right)^2 \left[S_1^2 + S_2^2\right] E_\gamma^3, \tag{28}$$

where $x_0 = x_{tp} e^{\frac{-\gamma}{2}\frac{t_{CN}}{2}}$ and

$$S_1 = \frac{\Gamma^\downarrow/2}{(E_\gamma - E_0)^2 + (\Gamma^\downarrow/2)^2} - \frac{\Gamma^\downarrow/2}{(E_\gamma + E_0)^2 + (\Gamma^\downarrow/2)^2}$$
$$S_2 = \frac{(E_\gamma + E_0)}{(E_\gamma + E_0)^2 + (\Gamma^\downarrow/2)^2} - \frac{(E_\gamma - E_0)}{(E_\gamma - E_0)^2 + (\Gamma^\downarrow/2)^2} \tag{29}$$

with $E_\gamma = \hbar\omega$ and $E_0 = \hbar\omega_0$. We remind that the Fourier transform $x_1(\omega)$ has been calculated by starting from Eqs. (19) and (20), with $\psi = 0$. Equation (28) represents the extra dipole contribution. We introduce later the dependence from the entrance channel conditions by parameterizing x_0, $\Gamma^\downarrow = \hbar\gamma$, and E_0.

We can try to introduce the time in Eq. (24). In this way we obtain the total time-dependent γ rate $dR/dE_\gamma(t)$ as the sum of the direct contribute γ rate $dR^{(1)}/dE_\gamma(t)$ and the statistical one $dR^{(r)}/dE_\gamma$.

$$\frac{dR}{dE_\gamma}(t) = \frac{dR^{(1)}}{dE_\gamma}(t) + \frac{dR^{(r)}}{dE_\gamma}. \tag{30}$$

We have extrapolated the constant term $dR^{(r)}/dE_\gamma$ in Eq. (25), whereas we can introduce the time in the first term of Eq. (24) starting from the following simple semiclassical considerations.

As it is well known from classical electrodynamics, the instantaneous emitted power is proportional to the square of the acceleration $\{[\ddot{x}_1(t)]^2$ in our case$\}$. Then, starting from Eq. (19) and supposing a very small dissipation constant γ, it is very easy to verify that

$$[\ddot{x}_1(t)]^2 \propto \sin^2[\omega_0(t - t_{CN}/2)]e^{-\gamma t}. \tag{31}$$

If we average on time the first factor we obtain $< [\ddot{x}_1(t)]^2 > \propto e^{-\gamma t}$. We obtain for the direct contribution γ rate

$$\frac{dR^{(1)}}{dE_\gamma}(t) = \gamma e^{-\gamma(t - t_{CN}/2)} \frac{dP^{(1)}}{dE_\gamma}; \quad t \geqslant t_{CN}/2, \tag{32}$$

where the constant $\gamma e^{\gamma t_{CN}/2}$ has been introduced so that $\int_{t_{CN}/2}^{\infty} \frac{dR^{(1)}}{dE_\gamma}(t)dt = \frac{dP^{(1)}}{dE_\gamma}$. The complete expression for the total γ rate can be written by adding to Eq. (32) the thermal pre-equilibrium contribution [see Eq. (25)]. We have

$$\frac{dR}{dE_\gamma}(t) = \frac{dR^{(1)}}{dE_\gamma}(t) + [1 - e^{-\gamma(t - t_{CN}/2)}]\frac{1}{\hbar}\frac{E_\gamma^2}{(\pi\hbar c)^2}\sigma_{abs} e^{-E_\gamma/T}. \tag{33}$$

We note the presence of a corrective factor to the second term (the statistical one). In particular we obtain this term by multiplying $dR^{(r)}/dE_\gamma$ in Eq. (25) by the factor $3[1 - e^{-\gamma(t - t_{CN}/2)}]$; where the factor 3 was inserted taking into account that the statistical-type contribution acts along all the three axes, whereas the direct contribution $dR^{(1)}/dE_\gamma(t)$ acts only along the beam axis. Moreover, the factor $[1 - e^{-\gamma(t - t_{CN}/2)}]$ takes into account the delay effect due to the start time of the fictitious random force $F_r(t)$ that, with a good approximation, we have fixed at $t = t_{CN}/2$. The introduction of this delay factor will be clarified in the next section where we will try to rewrite Eq. (33) following a full GDR phonon picture. In particular, it will be shown that it is possible to extend the phonon model [1] also at the pre-CN phase ($t_{CN}/2 \leqslant t < t_{CN}$). Then, by comparing Eq. (33) with the correspondent extended phonon-model equation, we will justify the introduction of this factor.

We observe that formula (33) consists of only two terms (the direct and the statistical term) and only in the latter the temperature T is present. This structure reflects Eq. (22). In fact from the deduction of this equation it follows that no interference term is present. The two terms in Eq. (33) are due to different physical mechanisms. Whereas the statistical term, due to the fluctuating dipolar excitation, is a typical incoherent contribution, the direct term is due to a coherent oscillation [4] of dynamical nature that is independent by the temperature T. For the same reasons the first term is characterized by a resonant function $(S_1^2 + S_2^2)$ that is quite different from the standard Lorentzian shape of the second term.

The availability of a time-dependent formula [Eq. (33)] represents an interesting opportunity for future developments, mainly because of the possibility of inserting this formula into a Monte Carlo cascade code to perform time-dependent simulations [2,15,16]. In fact only through these techniques it is possible to take into account in a correct and easy way many effects that Eq. (28) does not include. Some of them are (i) possible small variations of $\Gamma^\downarrow$ and E_0 as a function of time, (ii) the GDR escape width $\Gamma^\uparrow$, (iii) the temporal decrease of the ratio NZ/A due to the strong preequilibrium emission for high incident energy, and (iv) the γ-fission competition in the case of heavy colliding nuclei.

To obtain the extra yield contribution probability as a function of the incident beam energy, the formula (32) has been numerically integrated over E_γ and analytically over the time, so the extra yield contribution can be divided into two parts [the pre-CN contribution ($t_{CN}/2 \leqslant t < t_{CN}$) and the CN one ($t \geqslant t_{CN}$)], which are characterized by a different parametrization as shown in the following. The calculations were performed for the systems $^{16}O + {}^{98}Mo$ and $^{40}Ca + {}^{100}Mo$. Note that these systems were experimentally

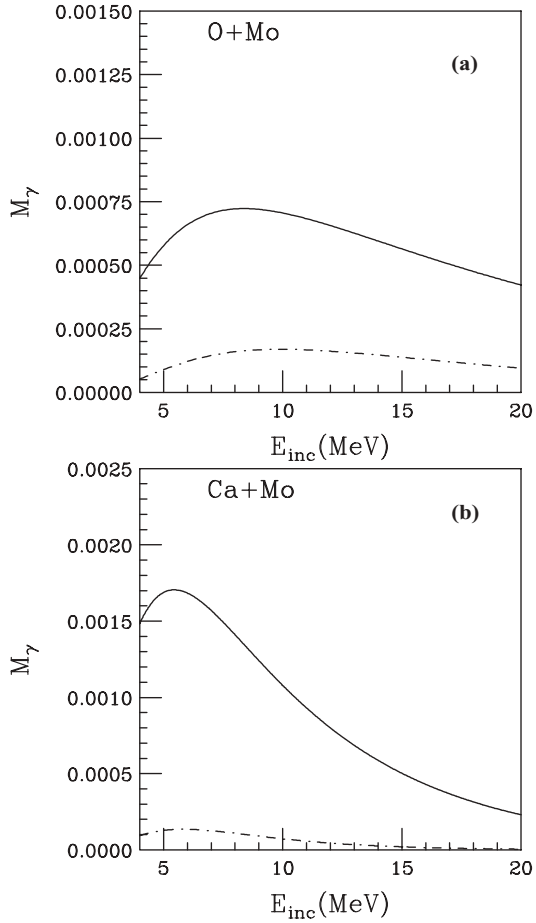

FIG. 4. Extra photon multiplicity as a function of the incident beam energy for the two studied systems (see text): total extra photon multiplicity (full line), and CN extra photon multiplicity (dashed line).

studied in Refs. [5,6]. The results of our calculations are plotted in Figs. 4(a) and 4(b).

In Fig. 4(a) the extra yield contribution (full line) versus the incident beam energy is plotted for the system $^{16}O + {}^{98}Mo$. The dashed line shows the contribution relative to the instants following the compound nucleus formation time ($t \geqslant t_{CN}/2$). In Fig. 4(b) the same probabilities are evaluated for the system $^{40}Ca + {}^{100}Mo$.

We note a general agreement of our total extra yield contribution (full lines) with the same quantity evaluated in Ref. [3]. In particular we have a very nice agreement in the $^{16}O + {}^{98}Mo$ case. Moreover, the typical "rise and fall" behavior, which was observed in Ref. [3], is well reproduced in both cases. These comparisons confirm the accurancy of our model [Eqs. (28) and (33)], taking into account that our formula [Eq. (28)] is based on the same "bremsstrahlung" approach used in Ref. [3].

In Fig. 5 we show the ratio between total pre-equilibrium and total statistical γ multiplicity as a function of the incident beam energy for the two studied systems. We evaluate the total statistical GDR contribution by using a very simple cascade model that takes into account only γ and neutron channels. We observe as in this case the "rise and fall" behavior is hidden by

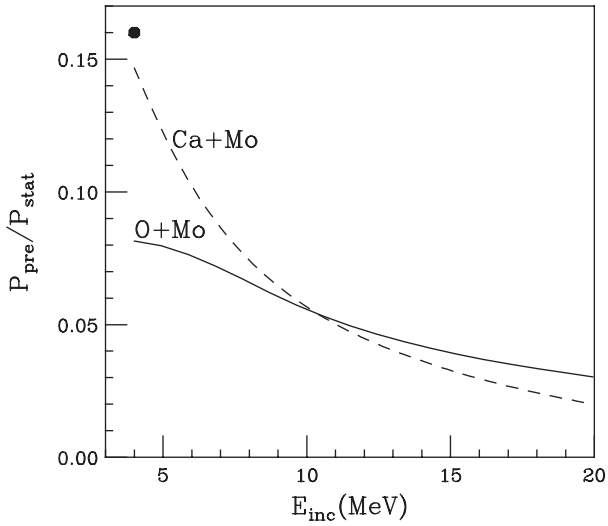

FIG. 5. Ratio of total pre-eqilibrium to total statistical GDR γ-ray emission for the two studied systems (see text): $^{16}O + {}^{98}Mo$ (full line); $^{40}Ca + {}^{100}Mo$ (dashed line). The full circle, relative to the reaction $^{40}Ca + {}^{100}Mo$, represents the experimental data.

the statistical contribution of the daughter nuclei. In the case of Ca + Mo reaction at $4A$ MeV we can compare our results with the experimental data [5]. The agreement is quite good.

Let us now discuss the parametrization used for x_0, $\Gamma^{\downarrow} = \hbar\gamma$ and the centroid E_0 energy in Eqs. (28) and (33).

The spreading width $\Gamma^{\downarrow}$ has been parametrized by using $\Gamma^{\downarrow}_{E^*} = 4.8 + 0.0026^*(E^*)^{1.6}$ (empirical formula [17] used for the systems close to the Sn^*). In particular for $t \geqslant t_{CN}$ we calculate $\Gamma^{\downarrow}_{E^*}$ with the compound nucleus excitation energy $E^* = E_{cm} + Q$, whereas for $t_{CN}/2 \leqslant t < t_{CN}$ we use $\langle E^* \rangle = \int_{t_{CN}/2}^{t_{CN}} E^*(t)dt \cong 0.6E^*$[4]. In this way we roughly take into account the influence of the quasiequilibrium configuration on the $\Gamma^{\downarrow}$ during the pre-CN phase.

The amplitude $x_0 = x_{tp} e^{\frac{-\gamma}{2}\frac{t_{CN}}{2}}$ has been computed by using $\gamma = \Gamma^{\downarrow}_{\langle E^* \rangle}/\hbar$; and the touching point distance

$$x_{tp} = \frac{Z_p Z_t}{NZ}\left|\frac{N_p}{Z_p} - \frac{N_t}{Z_t}\right|(R_p + R_t);$$
$$R_{p,t} = r_0 A_{p,t}^{1/3}; \quad r_0 = 1.2 \text{ fm}. \tag{34}$$

Moreover, the compound nucleus formation time (t_{CN}) is parametrized as a function of the incident beam energy per nucleon by using

$$t_{CN} = \frac{581.6}{E_{inc}/A_p}. \tag{35}$$

This expression was obtained by fitting the compound nucleus formation time values extrapolated in Ref. [2] for the system $^{16}O + {}^{98}Mo$ with the functional behavior $t_{CN} \propto \frac{1}{E_{cm}/A_p}$ (see

[4]We use $E^*(t) = E^*(1 - e^{-2t/t_{CN}})$. This kind of behavior can be justified by solving a Boltzmann kinetic equation for the impulse distribution function $g_{p,t}(\vec{p})$ of the projectile (target) nucleons, after a simple linearization on the collision integral.

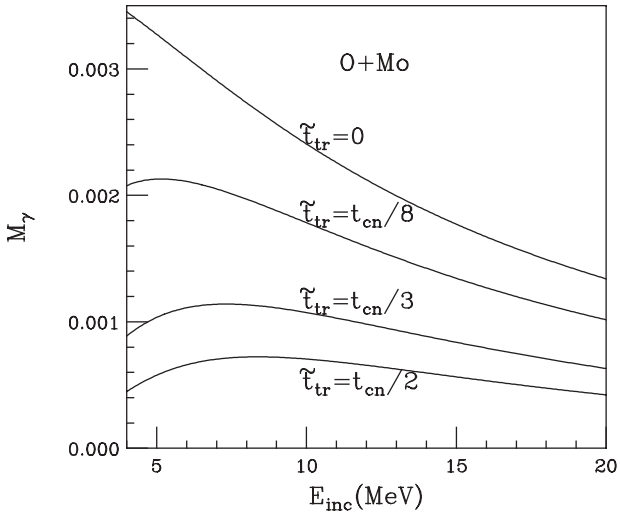

FIG. 6. Total extra photon multiplicity as a function of the incident beam energy for the system $^{16}O + {}^{98}Mo$; by assuming that the transition time occures at different values.

Ref. [18]). Finally, for the centroid energy E_0 we use the standard well-known expression $E_0 = 31.2 \times A^{-1/3} + 20.6 \times A^{-1/6}$ MeV.

Let us focus now our attention on the origin of the "rise and fall" behavior. For this reason in Fig. 6 we have plotted the total extra yield probability for the system $^{16}O + {}^{98}Mo$ by supposing that the transition time $\tilde{t}_{tr}$ occurs at the following different values $\tilde{t}_{tr} = t_{CN}/n; n = 2, 3, \ldots 8, \ldots \infty$. As you can see the typical "rise and fall" behavior disappear when $n \to \infty$. In other words, if we suppose that the collective response (in the sense of proper GDR mode) occurs instantaneously, just after the strong absorption configuration (that is, when $\tilde{t}_{tr} \to 0$), the total extra yield radiation probability moves away from its natural "rise and fall" trend, acquiring very large values. This shows that the typical behavior in question is strictly connected to the transition in frequency that is due to the soft-to-hard mode transition discussed in the previous section.

In particular we can say that this behavior is due to the interplay of three effects:

(i) Following classical electrodynamics the very low frequency of the soft dipole ensures the negligibility of γ emission during the first $t_{CN}/2$ fm/c.
(ii) The compound nucleus formation time strongly decreases when the beam incident energy grows.
(iii) The fast increase of the spreading width $\Gamma^{\downarrow} = \hbar\gamma$ with the beam incident energy.

IV. THE EXTENDED PHONON MODEL

The starting point of the model presented in the previous section consists in the sharp cut-off approximation [Eqs. (11) and (14)]. In particular, we assume a full GDR behavior for $t \geqslant t_{CN}/2$, neglecting in this range of time the effects of the molecular component. This approximation is based on the soft-to-hard mode transition studied in Sec. I. In fact, the transition generates a strong attenuation of the molecular component for $t \geqslant \tilde{t}_{tr} = t_{CN}/2$. These considerations suggest the possibility of extending the GDR phonon model [1] to include the pre-CN phase $(t_{CN}/2, t_{CN})$.

As is well known, the original GDR phonon model, developed by Chomaz *et al.* [1], predicts the extra yield γ rays due to the CN phase $(t \geqslant t_{CN})$. It consists in a simple model of a GDR phonon gas interacting with the CN. In this approach the time-dependent γ rate during the CN phase is given by

$$\frac{dR}{dE_\gamma}(t) = n_{CN} e^{-\gamma(t-t_{CN})}\gamma_\gamma + [1 - e^{-\gamma(t-t_{CN})}]\frac{\lambda}{\gamma}\gamma_\gamma, \quad (36)$$

where n_{CN} is the mean number of excited GDR phonons at the time when the CN is formed, $\gamma = \Gamma^{\downarrow}/\hbar$ and $\lambda = \Gamma_{feed}/\hbar$ is the unit time probability to have some feeding from the CN heat bath. Finally, γ_γ is the partial width for photon emission [1]. We note that Eq. (36) works in the range of time between the CN formation time [$t = t_{CN}$ in Eq. (36)] up to the decay of the CN itself.

As just discussed, the possibility to preserve the standard GDR scheme during the pre-CN phase permits us to extend the quantum picture also during this phase, obviously by introducing some approximations. We note that also in terms of the Brink-Axel hypothesis [19] this extension is acceptable.

Within the interval $(t_{CN}/2, t_{CN}/2 + \tau_{ev})$ we can directly write for the extended phonon model

$$\frac{dR}{dE_\gamma}(t) = n_0 e^{-\gamma(t-t_{CN}/2)}\gamma_\gamma + [1 - e^{-\gamma(t-t_{CN}/2)}]\frac{\lambda}{\gamma}\gamma_\gamma, \quad (37)$$

where now n_0 is the mean number of GDR phonons at $t_{CN}/2$.

We observe that the ratio $\frac{\lambda}{\gamma}$ in Eq. (37) should be in effect time dependent during the pre-CN phase $(t_{CN}/2, t_{CN})$, but in this equation this ratio coincides with its equilibrium value: $\lambda/\gamma \cong 3\rho(E^* - E_{GDR})/\rho(E^*) \approx 3\exp(-E_{GDR}/T)$. This is the main approximation introduced in the extension of the phonon model. We stress that this approximation has the same meaning of the approximation done in the pre-equilibrium model of Sec. III about the features of the random force $F_r(t)$.

In Eqs. (36) and (37) the partial width γ_γ is given by (see also Ref. [2])

$$\gamma_\gamma = \frac{1}{\hbar}\frac{\rho(E^* - E_\gamma)}{\rho(E^* - E_{GDR})}\frac{E_\gamma^2}{(\pi\hbar c)^2}\frac{\sigma_{abs}}{3} \cong \frac{1}{\hbar}e^{\frac{E_{GDR}-E_\gamma}{T}}\frac{E_\gamma^2}{(\pi\hbar c)^2}\frac{\sigma_{abs}}{3} \quad (38)$$

As discussed in Sec. III the coincidence of the second term of Eq. (37) with the second term of Eq. (33) justifies the validity of the introduction of the delay factor $[1 - e^{-\gamma(t-t_{CN}/2)}]$ in Eq. (33).

By comparing the model of Sec. III [Eq. (33)] with the extended phonon model [Eq. (37)] we note that in the last one, unlike that in our pre-equilibrium model (Sec. III), the temperature T and the Lorentzian function are present in both terms of the Eq. (37). This is due to the fact that the phonon model (and its extended version) neglects the coherent effects and the dynamical nature of the pre-equilibrium contribution (see Sec. III). Therefore, for a correct use of the phonon model

it is necessary to suppress the factor $\exp[(E_{\mathrm{GDR}} - E_\gamma)/T]$ in the evaluation of the partial decay width γ_γ [Eq. (38)] relative to the first term. One can infer this conclusion by comparing the two models. In fact, starting from our pre-equilibrium model it is possible to recover the extended phonon model with the help of some approximations. In conclusion the comparison of the two models gives hints on the operative use of the phonon model, clarifying how the partial decay width should be calculated in this model.

V. SUMMARY AND CONCLUSIONS

This work focuses on the role played by the dynamic features of the dipole mode on the γ-emitting properties of a compound nuclear system produced in a charge asymmetric fusion entrance channel.

By using the microscopic transport BNV approach we have analyzed the dipole evolution in the reaction $^{16}\mathrm{O} + {}^{98}\mathrm{Mo}$, which presents a charge asymmetry in the entrance channel. The BNV analysis shows how in effect the dynamical dipole mode is a mixing of two modes: the molecular (soft mode) and the GDR (hard mode). Moreover, we observe a typical transition between the two modes that explains the main properties of the dynamical dipole. The correspondent transition time occurs at about half of the compound nucleus formation time ($t \approx t_{\mathrm{CN}}/2$).

Roughly speaking this instant divides the time scale in two stages. The very early stage ($t < t_{\mathrm{CN}}/2$) is dominated by the molecular mode, which is more similar to a soft GDR where a fluid of $^{16}\mathrm{O}$ oscillates against a fluid of $^{98}\mathrm{Mo}$. So $t = t_{\mathrm{CN}}/2$ can be approximatively considered coincident with the instant correspondent to the start of the well-known GDR mode.

The molecular mode is characterized by a frequency lower than the GDR mode one. Consequently, a transition trend is also observed in the oscillation frequency of the total dipole, characterized by the same transition time ($t \cong t_{\mathrm{CN}}/2$).

The observed soft-to-hard mode transition permits us to clarify the γ-emitting properties characterizing this kind of reaction. In particular, as widely discussed at the end of Sec. III, the transition clarifies the origin of the rise and fall behavior of the extra γ yield versus the incident beam energy.

In this work we have developed a new model based on the classic bremsstrahlung approach to compute the total γ-ray emission probability. The model nicely reproduces the rise and fall behavior.

The formalism obtained within our model could be very useful for future calculations related to the dynamical dipole mode. In particular, by inserting the obtained time-dependent formula [Eqs. (28)–(33)] into Monte Carlo statistical code [2,15,16] we will have a better comparison with experimental data because of the possibility of taking into account the competition of the γ emission with different pre-equilibrium effects. By using these Monte Carlo procedures our model could be very useful in the study of cooling effects due to the strong pre-equilibrium γ emission in the reactions leading to superheavy elements.

ACKNOWLEDGMENTS

We thank Professor A. Bonasera and Dr. A. Musumarra for useful discussions.

[1] Ph. Chomaz *et al*., Nucl. Phys. **A563**, 509 (1993).
[2] V. Baran *et al*., Nucl. Phys. **A679**, 373 (2001).
[3] V. Baran, D. M. Brink, M. Colonna, and M. DiToro, Phys. Rev. Lett. **87**, 182501 (2001).
[4] M. Papa *et al*., Phys. Rev. C **68**, 034606 (2003).
[5] S. Flibotte *et al*., Phys. Rev. Lett. **77**, 1448 (1996).
[6] M. Cinausero *et al*., Nuovo Cimento A **111**, 613 (1998).
[7] F. Amorini *et al*., Phys. Rev. C **58**, 987 (1998).
[8] TWINGO code, A. Guarnera, Ph.D. thesis, University of Caen, 1996.
[9] A. Bonasera *et al*., Phys. Lett. **B221**, 233 (1989).
[10] A. Bonasera *et al*., Phys. Rep. **243**, 1 (1994).
[11] V. Greco, Ph.D. thesis, University of Catania, 1997 (unpublished); V. Greco *et al*., Phys. Rev. C **59**, 810 (1999).
[12] M. Papa *et al*., Eur. Phys. J. A **4**, 69 (1999).
[13] J. D. Jackson, *Classical Electrodynamics* (Wiley, New York, 1962).
[14] L. D. Landau and E. M. Lifshitz, *Statistical Physics* (Pergamon Press, New York, 1989), p. 386.
[15] M. Cabibbo *et al*., Nucl. Phys. **A637**, 374 (1998).
[16] M. Cabibbo, Ph.D. thesis, University of Catania, 1998 (unpublished).
[17] Chakrabarty *et al*., Phys. Rev. C **36**, 1886 (1987).
[18] C. Toepffer and C. Y. Wong, Phys. Rev. C **25**, 1018 (1982).
[19] D. M. Brink, Ph.D. thesis, Oxford University, 1955; P. Axel, Phys. Rev. **126**, 671 (1962).